[9]W. R. Graham and G. Ehrlich, J. Phys. F 4, 2212 (1974).
[10]D. A. Reed and G. Ehrlich, Philos. Mag. 32, 1095 (1975).
[11]D. W. Bassett, in *Surface and Defect Properties of Solids*, edited by M. W. Roberts and J. M. Thomas (Chemical Society, London, 1973), Vol. 2, p. 34.
[12]D. W. Bassett, J. Phys. C 4, 2491 (1976).
[13]T. T. Tsong and R. J. Walko, Phys. Status Solidi (a) 12, 111 (1972).
[14]D. Elwell and H. J. Scheel, *Crystal Growth from High Temperature Solutions* (Academic, New York, 1975).
[15]J. M. Blakely, Prog. Mater. Sci. 10, 395 (1963); G. E. Rhead, Scr. Metallogr. 6, 47 (1972).
[16]G. Ertl and J. Küppers, *Low Energy Electrons and Surface Chemistry* (Verlag Chemi, Weinheim, 1974).
[17]H. P. Bonzel, CRC Crit. Rev. Solid State Sci. 6, 171 (1976); G. E. Rhead, Surf. Sci. 47, 207 (1975).
[18]D. A. Reed and G. Ehrlich, J. Chem. Phys. 64, 4616 (1976).
[19]Since the completion of this work, a study of the 1D motion of Re dimers of W(211) has been published, in which a proper analysis is given; see Stolt, W. R. Graham, and G. Ehrlich, J. Chem. Phys. 65, 3206 (1976).
[20]E. W. Montroll and G. Weiss, J. Math. Phys. (N.Y.) 6, 167 (1965); H. Scher and M. Lax, Phys. Rev. B 7, 4491 (1973); E. W. Montroll and H. Scher, J. Stat. Phys. 9, 101 (1973); M. F. Shlesinger, *ibid.*, 10, 421 (1974).
[21]U. Landman, E. W. Montroll, and M. F. Shlesinger, Proc. Nat. Acad. Sci., U. S. A. (February, 1977). For a discussion of random walk with internal states, see also E. W. Montroll, J. Math. Phys. (N.Y.) 10, 753 (1969).
[22]The function $g(V)$ describes the bias-field dependence of the activation energy [see Ref. 13 and S. Nisigaki and S. Nakamura, Jpn. J. Appl. Phys. 15, 1647 (1976)].
[23]U. Landman, E. W. Montroll, and M. F. Shlesinger, to be published.
[24]From a comparison of results obtained from the analysis of biased and bias-free data, the effect of external fields on the transition rates could be investigated.

Self-Consistent Approximation to the Hubbard Model*

E. N. Economou and C. T. White†
Department of Physics, University of Virginia, Charlottesville, Virginia 22901
(Received 20 October 1975; revised manuscript received 27 December 1976)

The Hubbard model is studied by employing a random-potential approximation, which incorporates the effects of magnetic ordering and dynamical processes. Comparison of our results to existing data on one-dimensional systems shows that the present approximation is very accurate over the whole range of values of the physical parameters.

Hubbard,[1] in his treatment of the Hamiltonian

$$\hat{\mathcal{H}} = \sum_{i\sigma} \epsilon_0 \hat{n}_{i\sigma} + \sum_{ij\sigma} V_{ij} \hat{a}_{i\sigma}^{\dagger} \hat{a}_{j\sigma} + U \sum_i \hat{n}_{i\uparrow} \hat{n}_{i\downarrow}, \quad (1)$$

replaced the last term by a one-body random potential

$$U \hat{n}_{i\uparrow} \hat{n}_{i\downarrow} \approx \epsilon_{i\sigma} \hat{n}_{i\sigma}, \quad (2)$$

where $\epsilon_{i\sigma}$ was taken as U or 0 with equal probability. In Eq. (1), the sites $\{i\}$ form a lattice, σ takes two values [down ($\downarrow$) or up ($\uparrow$)], ϵ_0 is a constant, V_{ij} is usually taken (for simplicity) as a constant V when i and j are nearest neighbors and zero otherwise, $\hat{a}_{i\sigma}^{\dagger}$ and $\hat{a}_{i\sigma}$ are creation and annihilation operators of a local state at the site i with spin σ, and $\hat{n}_{i\sigma} = \hat{a}_{i\sigma}^{\dagger} \hat{a}_{i\sigma}$. Subsequently,[2] $\epsilon_{i\sigma}$ was taken as $\frac{1}{2}U(1+\tilde{\mu})$ or $\frac{1}{2}U(1-\tilde{\mu})$, where $\tilde{\mu}$ was obtained self-consistently and was interpreted as the size of a local moment, the z component of which can take on two values, $\pm\tilde{\mu}$. This approach to the problem, though an improvement over the original Hubbard treatment, misses two important features of the model: (1) The influence of the magnetic ordering (MO) on the electronic properties is omitted except for the limiting cases of perfect order or no order at all; thus, this effect is treated satisfactorily only at the extreme temperatures, $T=0$ or $T=\infty$. (ii) The dynamic processes (DP), which allow μ_{iz} to change with time from $+\tilde{\mu}$ to $-\tilde{\mu}$ and vice versa, are neglected; the local moments are "frozen" in a particular configuration.

In the formalism summarized below, MO (equivalent to an Ising coupling) is incorporated in a self-consistent way, and its effect on the electronic structure is included. Furthermore, it is argued that DP amount to replacing the Ising by a Heisenberg coupling. With the present incorporation of MO and DP, one can provide strong evidence that a satisfactory understanding of the behavior of the Hubbard model has been achieved.

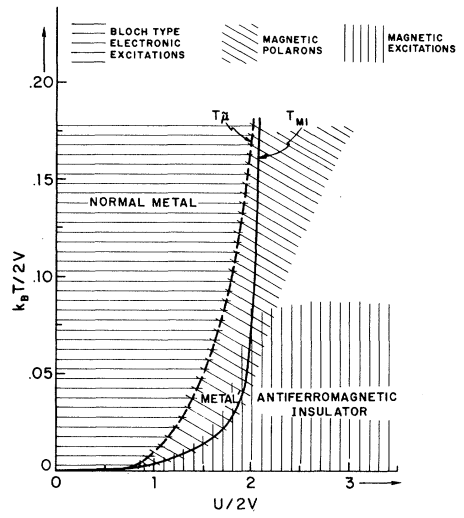

FIG. 1. Diagram for the 1D Hubbard model showing the nature of low-lying elementary excitations: At T_{MI} a metal-insulator transition takes place; and at $T_{\tilde{\mu}}$ the local moments almost disappear.

We outline first our way of incorporating MO, without regard to DP, which will be included later. Because of Eq. (2), the Hubbard Hamiltonian has been reduced to a one-body random Hamiltonian. The random variables $\{\epsilon_{i\sigma}\}$ are assumed to have the probability distribution

$$\mathcal{P}(\epsilon_{i\uparrow},\epsilon_{i\downarrow}) = \tfrac{1}{2}\delta(\epsilon_{i\uparrow}-\epsilon_{\uparrow}^{A})\delta(\epsilon_{i\downarrow}-\epsilon_{\downarrow}^{A}) + \tfrac{1}{2}\delta(\epsilon_{i\uparrow}-\epsilon_{\uparrow}^{B})\delta(\epsilon_{i\downarrow}-\epsilon_{\downarrow}^{B}), \quad (3)$$

with $\epsilon_{\uparrow}^{A}=\epsilon_{\downarrow}^{B}=\frac{1}{2}U(1-\tilde{\mu})$ and $\epsilon_{\downarrow}^{A}=\epsilon_{\uparrow}^{B}=\frac{1}{2}U(1+\tilde{\mu})$ for the half-filled case examined here. In addition, a MO parameter P is introduced such that P gives the probability of finding a local moment up, given that a nearest-neighboring moment is down. This MO is equivalent to an Ising coupling.[3] Thus, the probability distribution of $\{\epsilon_{i\sigma}\}$ is characterized by two yet-undertermined parameters $\tilde{\mu}$ and P. We have developed techniques for calculating average densities of states,[4] $\rho(E)$, for such random systems. Having P and $\rho(E;\tilde{\mu},P)$ one can obtain the free energy $F(T;\tilde{\mu},P)$. The quantities $\tilde{\mu}$ and P can then be determined by minimizing $F(T;\tilde{\mu},P)$. Note that P is a function of βJ_0 alone, where J_0 is the coupling constant of the equivalent Ising Hamiltonian, $H_I=-J_0\sum_i\sigma_{iz}\sigma_{i+1z}$; for the one-dimensional (1D) case $P=e^{-\beta J_0}/(e^{-\beta J_0}+e^{\beta J_0})$. Thus, for each point of the U-T plane (see Fig. 1) we can obtain $\tilde{\mu}$, J_0, and $\rho(E;T)$, and consequently determine the physical behavior of the system.

Here we describe briefly results found by applying to a 1D lattice the formalism outlined above. The 1D system was chosen in order to check the quantitative accuracy of our scheme against existing exact results and numerical data. Our results for higher-dimensional lattices will be presented elsewhere.

At $T=0$, we find that the system possesses perfect antiferromagnetic order ($P=1$). The moment $\tilde{\mu}$ increases monotonically from zero at $U/2V=0$ to 1 at $U/2V=\infty$; as $U/2V\to 0$, $\tilde{\mu}\to(16V/U)\exp(-2\pi V/U)$. The density of states exhibits a gap, $E_g=U\tilde{\mu}$, separating two main sub-bands consisting of Bloch states with periodicity twice the lattice spacing.

As the temperature T is raised, the perfect MO is disrupted by occasional magnetic "defects." Electrons can be trapped around these "defects" creating "impurity" levels in the gap. These "defect" states can be termed localized magnetic polarons. Further rise in T increases the concentration of magnetic "defects" and the magnetic polaron levels will be broadened to "impurity" subbands in the gap; eventually these impurity "subbands" merge with the main sub-bands.

For $U/2V\gtrsim 2$, a gap around the Fermi level remains for all temperatures and $\tilde{\mu}$ is roughly T independent. On the other hand, for $U/2V\lesssim 2$, the gap closes for $T\approx T_{MI}$ (see Fig. 1); furthermore, the moment $\tilde{\mu}$ and the magnetic coupling J_0 decrease with increasing T, and for $T\gtrsim T_{\tilde{\mu}}$ they are practically zero. For $T>T_{\tilde{\mu}}$, the system behaves as a normal metal adequately described by Hartree-Fock, Bloch states. For $T_{MI}\lesssim T\lesssim T_{\tilde{\mu}}$ we have a metal (in the sense that $\rho_F\neq 0$), but a peculiar one with the states around E_F being not of the Bloch type but rather of the magnetic polaron type; furthermore, the density of states around E_F exhibits considerable structure. We can characterize the behavior of our system for $U/2V\lesssim 2$ by saying that the low-lying elementary excitations are magnetic for low T and electronic (Bloch-type) for high T; for intermediate temperatures, they are magnetic polarons, i.e., a mixture of the two. Thus, a continuous transformation of the low-lying elementary excitations takes place with increasing T. This discussion is summarized in Fig. 1.

We now briefly consider how DP modify the above picture. DP allow the local moment at a site i to change from $\tilde{\mu}$ to $-\tilde{\mu}$ (or vice versa); at the same time the local moment at another site j should change from $-\tilde{\mu}$ to $\tilde{\mu}$ (or vice versa) to conserve the z component of the total spin. This process can be described by a Hamiltonian of the form $\Delta\hat{\mathcal{H}}=\sum_{ij}t_{ij}\sigma_i^{+}\sigma_j^{-}$, where σ_i^{+} and σ_j^{-} are the usual Pauli matrices. Thus, the incorporation

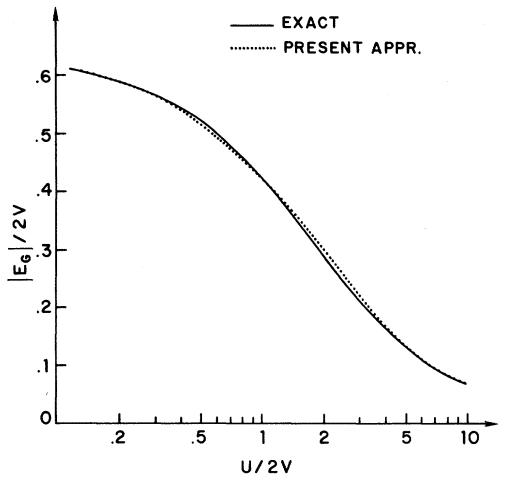

FIG. 2. The ground-state energy per electron for a half-filled 1D Hubbard model.

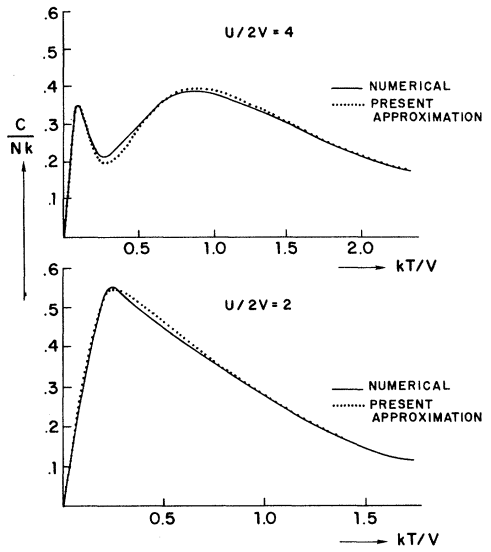

FIG. 3. Specific heat vs temperature for a half-filled 1D Hubbard model.

of DP is equivalent to adding $\Delta\hat{\mathcal{H}}$ to our random Hamiltonian; the Ising part of the latter, $\hat{H}_I = -J_0\sum_i \sigma_{iz}\sigma_{i+1z}$, will be transformed then to a Heisenberg part,[5] $\hat{H}_H = -J\sum_i \vec{\sigma}_i \cdot \vec{\sigma}_{i+1}$. Let us now examine the resulting changes in $\rho(E;\tilde{\mu},P)$. At $T=0$, zero-point magnons will be present, destroying the perfect magnetic ordering and creating tails around the edges of the two main sub-bands; thus the gap will be reduced. The magnetic polaron states appearing for $T>0$ will not be localized anymore, since each magnetic "defect," around which the electron is trapped, can now propagate through the crystal (as a magnon) dragging the bound electron with it. Such a propagation creates a sub-band out of each impurity level. This dynamical broadening is significant only at very low temperatures. For $T \gtrsim J/k_B$, it is mostly masked by "thermal" broadening, i.e., the creation of "impurity" sub-bands due to a high concentration of magnetic "defects." These changes in $\rho(E;T)$ are expected to modify the self-consistent values of $\tilde{\mu}$ and J at low T. The change in $\tilde{\mu}$ is insignificant except for very low values of $U/2V$ (i.e., $U/2V \lesssim 1$); however, we were not able to estimate it further. On the other hand, the value of J is modified significantly due mainly to the dynamical broadening of the "impurity" levels.

In our explicit calculations we took into account DP to the extent of (i) replacing the Ising coupling by the Heisenberg coupling, and (ii) renormalizing the magnetic coupling constant to a new value J by considering the effects of dynamical broadening on the impurity levels. However, $\tilde{\mu}$ and $\rho(E;T)$ were left unchanged. Figure 2 shows our result for the ground-state energy E_G per electron for the 1D case together with the exact results.[6] The small discrepancy around $U/2V \sim 2$ is due to a slight overestimate of the renormalized value of J; the discrepancy around $U/2V \sim 0.5$ is probably due to our omission of the effect of DP on $\tilde{\mu}$. In Fig. 3 we display our results for the specific heat versus T for two values of $U/2V$ together with the numerical data of Shiba.[7] The small differences can be possibly attributed to dynamical broadening of $\rho(E;T)$. We obtained equally satisfactory results for other physical quantities such as the magnetic susceptibility, which together with other quite interesting details concerning the behavior of the system in the region $T \lesssim T_{MI}$ and $U/2V \lesssim 1$ will be presented elsewhere.

In conclusion, the present approximation scheme produces a sensible physical picture and interpretation for the behavior of the Hubbard model. It reproduces the established results at the limiting metallic and atomic cases, and provides new insight into the little-understood region around the metal-insulator transition. The impressive quantitative agreement with the exact results and numerical data in the 1D case strongly suggests that the present formalism correctly incorporates all the basic physical ingredients for the first time.

Note that our approach can be applied straightforwardly to lattices of higher dimensionality and should work even better there. Also, it can be easily generalized to include external magnetic

fields, static randomness, etc. Thus, it is expected to become an important theoretical tool for studying many-body systems, especially narrow-band materials[8] (e.g., NiS) and impurity bands in crystalline semiconductors.[9]

*Work supported by National Science Foundation Grant No. DMR76-19458 and a University of Virginia computing grant.

†Present address: U. S. Naval Research Laboratory, Washington, D. C. 20375.

[1]J. Hubbard, Proc. Roy. Soc. London, Ser. A 281, 401 (1964).

[2]See, e.g., M. Cyrot, J. Phys. (Paris) 33, 125 (1972), and Philos. Mag. 25, 1031 (1972); P. Lacour-Gayet and M. Cyrot, J. Phys. C 7, 400 (1974); L. C. Bartel and H. S. Jarrett, Phys. Rev. B 10, 946 (1974).

[3]See, e.g. K. Huang, *Statistical Mechanics* (Wiley, New York, 1963).

[4]C. T. White and E. N. Economou, to be published.

[5]To arrive at this conclusion, one has to use the isotropy of our model; futhermore, it was assumed that the nearest-neighbor coupling is the dominant one.

[6]E. H. Lieb and F. Y. Wu, Phys. Rev. Lett. 20, 1445 (1968).

[7]H. Shiba, Prog. Theor. Phys. 48, 2171 (1972).

[8]We are using the present scheme to study the behavior of NiS; preliminary results agree well with experimental data and strongly suggest that a quantitative understanding of this interesting and controversial subject is at hand.

[9]Employing an extension of the approach presented here, we are currently investigating the long standing problem of negative magnetoresistance in impurity bands of crystalline semiconductors; our preliminary results are very encouraging.

Observations of Paired Electrostatic Shocks in the Polar Magnetosphere*

F. S. Mozer, C. W. Carlson, M. K. Hudson, R. B. Torbert, B. Parady, and J. Yatteau
Physics Department and Space Sciences Laboratory, University of California, Berkeley, California 94720

and

M. C. Kelley
School of Electrical Engineering, Cornell University, Ithaca, New York 14854

(Received 6 December 1976)

dc and ac plasma-density and vector–electric-field detectors on a polar orbiting satellite have measured spatially confined regions of extremely large ($\sim \frac{1}{2}$ V/m) electric fields in the auroral zone at altitudes below 8000 km. Such regions frequently have double structures of opposing electric fields containing characteristic and different wave spectra internal and external to themselves. These structures are identified as paired electrostatic shocks which are associated with electrostatic ion cyclotron wave turbulence.

The S3-3 satellite was launched during the summer of 1976 into a nearly polar orbit with perigee and apogee altitudes of 260 and 8050 km, respectively. On-board instruments have made the first *in situ* measurements of dc electric fields at auroral latitudes and altitudes where particle-acceleration, kilometric-radiation-generation, and anomalous-resistivity processes are thought to occur. The Berkeley experiment on this satellite measures the dc and ac plasma density and vector electric field. It has observed spatially confined regions of extremely large electric fields whose structure suggests paired electrostatic shocks that may be associated with particle acceleration, auroral arc formation, and wave production.

The electric-field detector consists of three orthogonal pairs of separated spheres whose measured potential differences yield three orthogonal components of the static or fluctuating electric field. Four of the spheres are located at the ends of four 18-m wire booms that are maintained in the satellite spin plane by centrifugal force. The remaining pair of spheres are oriented along the vehicle spin axis on 3-m rigid booms. By ground command, a sphere on a wire boom may be converted from the potential-measuring mode to a conventional Langmuir probe whose collected dc and ac currents yield the plasma density, temperature, and density fluctuations.

The magnitudes of electric fields expected at the satellite may be estimated by extrapolating the extensive ionospheric data[1] in altitude by assuming that magnetic-field lines are electric equipotentials. On this basis, the largest iono-